16th IEEE International Conference on Control Applications
Part of IEEE Multi-conference on Systems and Control
Singapore, 1-3 October 2007

State-Predictive Control of an Autonomous Blimp in the Presence of Time Delay and Disturbance

Hiroaki Fukushima*, Kazuyuki Kon*, Yasushi Hada†
Fumitoshi Matsuno*, Kuniaki Kawabata†, and Hajime Asama‡

Abstract— **In this paper, state-predictive control is applied to an autonomous blimp in the presence of time delay and disturbance. To this end, a state predictor to compensate time delay is constructed based on the separate-bias filters taking into account nonzero-mean disturbances. Experimental results show that constraint violations are reduced in model predictive control (MPC) with input and state constraints by compensating time delay. Also, flight experiments in the presence of the winds show that the steady-state error to disturbances are reduced as a result that the state prediction performance is improved by using separate-bias predictor. Moreover, MPC using soft bounds is applied for recovering constraint violoations due to disturbances.**

I. Introduction

Lighter Than Air vehicles (LTAs), also known as airships, have attracted much attention due to their potential utilization in surveillance, exploration, transportation and so on. Therefore, modeling and control methods of airships for autonomous flights have been actively studied in the last decade (see e.g. [1]-[5]).

Unlike most existing works, the authors have focused on autonomous flight control taking into account input constraints due to actuator saturations and output limitations from the viewpoint of safety[6]. Model predictive control (MPC), which is one of the few ways to handle input and state constraints explicitly[7]-[9], has been applied to an autonomous blimp, and indoor flight experiments have been performed to investigate the effectiveness. While the control performance has been improved by incorporating input and state constraints explicitly in controller design, the constraints have been violated in some examples[6].

One possible reason for such constraint violations is the transmission delay between the measurement system on the ground and the controller on the blimp. A common approach to deal with time delay is to incorporate delay into models for control optimization[7]. Another approach is state-predictive control, which predicts the state using a model and the past input to apply it to state feedback control for systems without delay[10]-[12].

In this paper, state-predictive control is applied to an autonomous blimp in the presence of time delay and disturbance. To this end, a state predictor to compensate time delay is constructed based on the separate-bias filters[13]-[15] taking into account nonzero-mean disturbance. Experimental results show that the constraint violation problem in [6] is overcome by compensating time delay in MPC. Also, flight experiments in the presence of the winds show that the steady-state error to disturbances are reduced as a result that the state prediction performance is improved by using separate-bias predictor. Moreover, MPC using soft bounds is applied for recovering constraint violoations due to disturbances.

*Department of Mechanical Engineering and Intelligent Systems, The University of Electro-Communications, 1-5-1 Chofugaoka, Chofu, Tokyo 182-8585, Japan.

†RIKEN (The Institute of Physical and Chemical Research), 2-1 Hirosawa, Wako, Saitama 351-0198, Japan.

‡RACE (Research into Artifacts, Center for Engineering), The University of Tokyo, 5-1-5 Kashiwanoha, Kashiwa, Chiba 277-8568, Japan.

II. Outline of blimp System

The unmanned blimp for our indoor experiments is depicted in Fig. 1. It has inertial sensors (three accelerometers, three magnetic gyroscopes, and an axis meter), actuators, a Linux PC, and batteries. It can communicate with a ground base using wavelan (IEEE 802.11b). The actuator consists of two cross-shaped vectored thrusters in the center of balance and two thrusters on the tail (Fig. 2). Localization of the blimp is based on the inertial sensors of the blimp and a position measurement system on the ground. TotalStation[16], which has an auto-tracking function, is used to measure the position of the blimp. See [5]-[6] for more detail on the experimental system.

As shown in Fig. 2, one pair of thrusters (A-B) is used for X direction on the body-fixed frame, and another pair (C-D) is used simultaneously for the Y-Z directions. The yaw angle is controlled by the tail rotors E-F, and the roll and pitch angles are not controlled since the blimp can move stably in an indoor environment. The control input variables U_X, U_Y, U_Z are defined as the thrust levels in X, Y, Z

Fig. 1. Blimp for experiments

1-4244-0443-6/07/$20.00 ©2007 IEEE.

directions, respectively. After compensating the deadzones of the thrusters as shown in [6], control input constraints in X, Y, Z directions are given as

$$|U_X(t)| \le 150, \quad \sqrt{U_Y^2 + U_Z^2} \le 150. \tag{1}$$

On the other hand, the thrust levels in x, y, z-directions on the global frame are defined as u_x, u_y, u_z.

In this paper, we only focus on position control from the initial position (x_0, y_0, z_0) to the origin. It is assumed that the yaw angle ψ with the initial condition $\psi_0 = 0$ is controlled independently by a given feedback law, so that $\psi \simeq 0$. Since this implies $(u_x, u_y, u_z) \simeq (U_X, U_Y, U_Z)$, it is reasonable to consider the same constraint as (1) for (u_x, u_y, u_z).

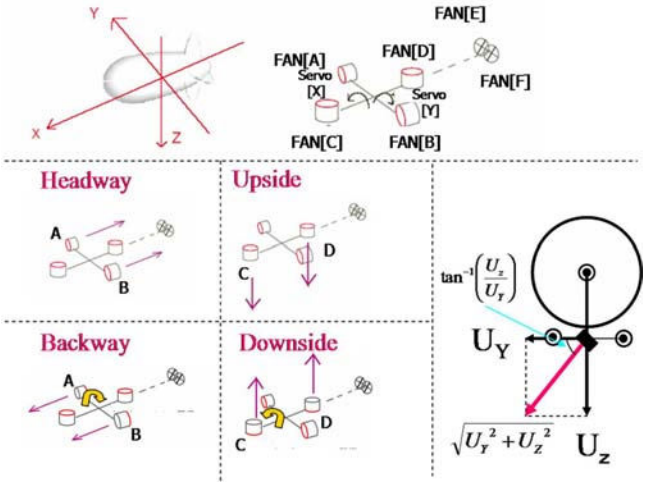

Fig. 2. Kinematics of the blimp actuators

III. State Prediction

In the same way as [6], state-space models are constructed independently in x, y, z directions based on the following simple motion equations:

$$\ddot{x} = b_1 u_x, \quad \ddot{y} = b_2 u_y, \quad \ddot{z} = b_3 u_z, \tag{2}$$

where b_1, b_2 and b_3 are positive numbers chosen based on step responses. Based on the motion equations in (2), state space models are constructed for $\xi_x := [x, \dot{x}]^T, \xi_y := [y, \dot{y}]^T, \xi_z := [z, \dot{z}]^T$ using the zero-order-hold discretization with sampling time $T_s = 0.8$. The difference from the model in [6] is that terms describing delay and disturbance are additionally introduced.

The model in x-direction with ℓ step delay is described as follows:

$$\begin{aligned} \xi_{x[k+1]} &= A_x \xi_{x[k]} + B_x u_{x[k-\ell]} + G_x w_{x[k]}, \\ x_{[k]} &= C_x \xi_{x[k]} + v_{x[k]} \end{aligned} \tag{3}$$

where $\xi_{x[k]} \in \mathbb{R}^2$ has Gaussian initial condition $\xi_{x[0]} \sim \mathcal{N}(\hat{\xi}_{x0}, \Sigma_x)$. It is assumed that $w_{x[k]} \in \mathbb{R}^r$ and $v_{x[k]} \in \mathbb{R}$ are zero-mean Gaussian white signals, which satisfy

$$E\left\{ \begin{bmatrix} w_{x[k]} \\ v_{x[k]} \end{bmatrix} [w_x^T{}_{[s]}, v_{x[s]}] \right\} = \begin{bmatrix} I_r & 0 \\ 0 & \Lambda_x \end{bmatrix}$$
$$E\{w_{x[k]} \xi_x^T{}_{[s]}\} = 0, \ E\{v_{x[k]} \xi_x^T{}_{[s]}\} = 0, \ k \ge s. \tag{4}$$

It is also assumed that A_x, B_x, C_x, G_x, Λ_x, Σ_x, $\hat{\xi}_{x0}$, and ℓ are given constants. Since the models and predictors for x, y, z directions are similarly described except for the difference of subscripts, we drop subscripts in the rest of the paper, whenever this does not lead to confusion.

The steady-state Kalman state estimator for the model as in (3) is described as follows[17]:

$$\hat{\xi}_{[k|k]} = \hat{\xi}_{[k|k-1]} + L(x_{[k]} - C\hat{\xi}_{[k|k-1]}) \tag{5}$$
$$\hat{\xi}_{[k+1|k]} = A\hat{\xi}_{[k|k]} + Bu_{[k-\ell]}, \tag{6}$$

where L is

$$L := PC^T(CPC^T + \Lambda)^{-1} \tag{7}$$

and P is obtained by solving the following algebraic Riccati equation (ARE):

$$P = A(P - PC^T(CPC^T + \Lambda)^{-1}CP)A^T + GG^T. \tag{8}$$

The initial condition is

$$\hat{\xi}_{[0|-1]} = \hat{\xi}_0, \quad u_{[-1]} = \cdots = u_{[-\ell]} = 0. \tag{9}$$

To compensate the time delay in (3), the state-predictive control methods decide $u_{[k]}$ based on ℓ-step predictor, which is the conditional mean

$$\hat{\xi}_{[k+\ell|k]} = A^\ell \hat{\xi}_{[k|k]} + \sum_{i=1}^{\ell} BA^{i-1} u_{[k+\ell-i]}, \tag{10}$$

instead of $\hat{\xi}_{[k|k]}$.

In this paper, we also consider the following model with nonzero-mean disturbance $b_{[k]}$ to take into account the effects of winds.

$$\begin{aligned} \xi_{[k+1]} &= A\xi_{[k]} + Bu_{[k-\ell]} + Gw_{[k]} + Hb_{[k]}, \\ b_{[k+1]} &= b_{[k]} + Dd_{[k]}, \\ x_{[k]} &= C\xi_{[k]} + v_{[k]} \end{aligned} \tag{11}$$

where $b_{[0]} \in \mathbb{R}^p$ is unknown, and $d_{[k]} \in \mathbb{R}^p$ is zero-mean Gaussian white noise. State estimation in the presence of unknown inputs have been actively studied since the end of 1960's[13]-[15]. Similarly to [13], we use the following augmented model:

$$\begin{aligned} \zeta_{[k+1]} &= \bar{A}\zeta_{[k]} + Bu_{[k-\ell]} + \bar{G}\bar{w}_{[k]}, \\ x_{[k]} &= \bar{C}\zeta_{[k]} + v_{[k]} \end{aligned} \tag{12}$$

where

$$\zeta := \begin{bmatrix} \xi \\ b \end{bmatrix}, \quad \bar{w} := \begin{bmatrix} w \\ d \end{bmatrix}, \quad \bar{C} := [C, 0] \tag{13}$$
$$\bar{A} := \begin{bmatrix} A & H \\ 0 & I \end{bmatrix}, \quad \bar{G} := \begin{bmatrix} G & 0 \\ 0 & D \end{bmatrix}. \tag{14}$$

It is assumed that the similar condition to (4) is satisfied for $\bar{w}$ and ζ.

$$E\left\{ \begin{bmatrix} \bar{w}_{[k]} \\ v_{[k]} \end{bmatrix} [\bar{w}^T{}_{[s]}, v_{[s]}] \right\} = \begin{bmatrix} I_{r+p} & 0 \\ 0 & \Lambda \end{bmatrix} \tag{15}$$
$$E\{\bar{w}_{[k]} \zeta^T{}_{[s]}\} = 0, \ E\{v_{[k]} \zeta^T{}_{[s]}\} = 0, \ k \ge s. \tag{16}$$

Similarly to (5)-(6), the state estimator for (12) is

$$\hat{\zeta}_{[k|k]} = \hat{\zeta}_{[k|k-1]} + \bar{L}(x_{[k]} - \bar{C}\hat{\zeta}_{[k|k-1]}) \quad (17)$$

$$\hat{\zeta}_{[k+1|k]} = \bar{A}\hat{\zeta}_{[k|k]} + \bar{B}u_{[k-\ell]}, \quad (18)$$

where

$$\bar{L} := \bar{P}\bar{C}^T(\bar{C}\bar{P}\bar{C}^T + \Lambda)^{-1} \quad (19)$$

and $\bar{P}$ is obtained by solving the following algebraic Riccati equation (ARE):

$$\bar{P} = \bar{A}(\bar{P} - \bar{P}\bar{C}^T(\bar{C}\bar{P}\bar{C}^T + \Lambda)^{-1}\bar{C}\bar{P})\bar{A}^T + \bar{G}\bar{G}^T. \quad (20)$$

The initial condition is set to

$$\hat{\zeta}_{[0|-1]} = \begin{bmatrix} \hat{\xi}_0 \\ 0 \end{bmatrix}, \quad (21)$$

since the initial value of b is unknown.

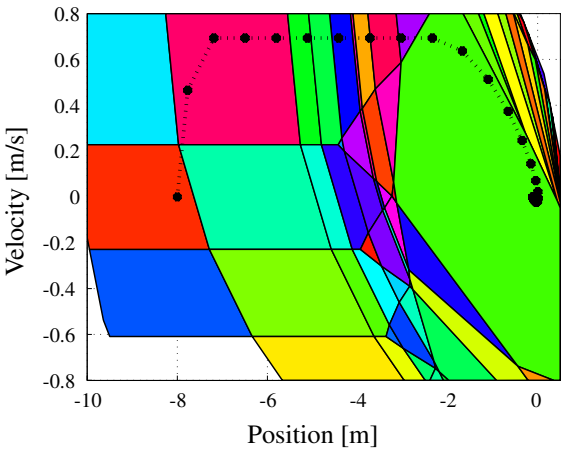

Fig. 3. Partitions in x direction using hard bound

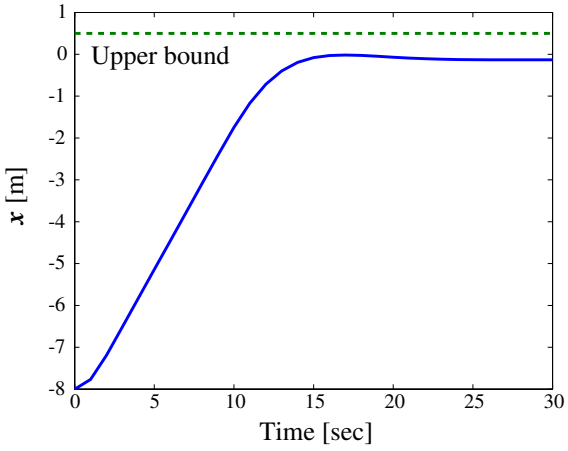

Fig. 4. Time plot of x in simulation

IV. Controller Design

Using the ℓ-step predictor $\hat{\xi}_{[k+\ell|k]}$ and the model

$$\hat{\xi}_{[k+\ell+1|k]} = A\hat{\xi}_{[k+\ell|k]} + Bu_{[k]}, \quad (22)$$

we design deterministic controllers. Controller design explicitly taking into account the disturbance terms in (3) or (11) is a future work.

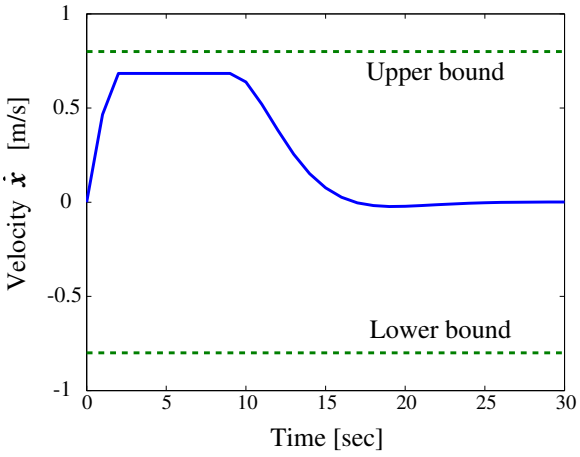

Fig. 5. Time plot of $\dot{x}$ in simulation

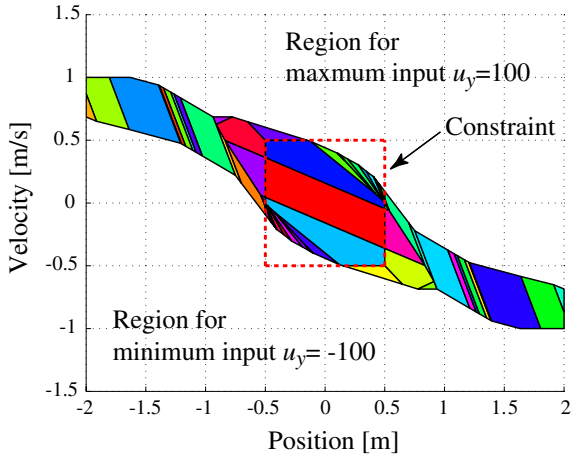

Fig. 6. Partitions in y direction using softbound

As mentioned in [6], since the linear state feedback law

$$u_{[k]} = -K\hat{\xi}_{[k+\ell|k]} \quad (23)$$

is difficult to handle input and state constraints especially for large initial states $\xi_{[0]}$, we consider the feedback law as

$$u_{[k]} = -K\hat{\xi}_{[k+\ell|k]} + \alpha_{[k]} \quad (24)$$

and choose $\alpha_{[k]}$ by MPC taking into account the constraints. Thus, the model in (22) for MPC can be written as

$$\xi_{[k+\ell+1|k]} = A_c\xi_{[k+\ell|k]} + B\alpha_{[k]} \quad (25)$$

$$A_c := A - BK. \quad (26)$$

MPC methods typically determine control input at each time step k based on finite horizon open-loop control optimization problems. A simple example of the optimization problem at k for a given $\hat{\xi}_{[k+\ell|k]}$ is

$$\min_{\hat{\alpha}} \sum_{\tau=k}^{k+N-1} \hat{\alpha}^2{}_{[\tau|k]} \quad (27)$$

subject to

$$\hat{\xi}_{[\tau+\ell+1|k]} := A_c\hat{\xi}_{[\tau+\ell|k]} + B\hat{\alpha}_{[\tau|k]} \quad (28)$$

$$\underline{\xi} \le \hat{\xi}_{[\tau+\ell+1|k]} \le \overline{\xi} \quad (29)$$

$$\underline{u} \le -K\xi_{[\tau+\ell|k]} + \hat{\alpha}_{[\tau|k]} \le \overline{u}, \quad (30)$$

where $\underline{\xi}, \overline{\xi}, \underline{u}, \overline{u}$ are the upper and lower bounds given in state and input constraints. The first element $\hat{\alpha}_{[k|k]}$ of the optimal solution is applied at each time step k, i.e. $\alpha_{[k]} = \hat{\alpha}_{[k|k]}$. The optimization problem above can be solved offline as piecewise affine feedback of the following form [8]-[9]:

$$v_{[k]} = \Phi_i \hat{\xi}_{[k+\ell|k]} + \Gamma_i, \quad if \quad \hat{\xi}_{[k+\ell|k]} \in \mathcal{P}_i \tag{31}$$

$$\mathcal{P}_i = \{\xi \in \mathbb{R}^2 | \; M_i \xi \leq E_i\}, \quad i = 1, \cdots, N_r, \tag{32}$$

where N_r is the number of the polytope regions $\mathcal{P}_i$.

In order to take into account disturbances and modeling errors, we adopt a robust MPC approach[9], which deals with the additive (deterministic) uncertainty δ as

$$\hat{\xi}_{[k+\ell+1|k]} = A_c \xi_{[k+\ell|k]} + B\alpha_{[k]} + \delta_{[k]}, \quad \delta_{[k]} \in \Delta. \tag{33}$$

The polytope Δ is simply chosen as

$$\Delta = \{\delta \in \mathbf{R}^2 | \; |\delta| \leq B\eta\} \tag{34}$$

to consider input disturbances, where η is a design parameter.

Fig. 3 shows partitions $\mathcal{P}_i$ for x direction with $\eta = 25$ in (34). The upper and lower bounds of the constraints in (29)-(30) are

$$\underline{\xi}_x = \begin{bmatrix} -0.8 \\ -10 \end{bmatrix}, \; \overline{\xi}_x = \begin{bmatrix} 0.8 \\ 0.5 \end{bmatrix}, \; \underline{u}_x = -100, \; \overline{u}_x = 100 \tag{35}$$

The feedback gain in (24) is chosen as $K_x = [-31.6, -117]$ based on LQ control. The dotted line in Fig. 3 shows a trajectory of ξ_x for $x_0 = -8$, which is obtained using Multi-Parametric Toolbox for MATLAB[18]. The time plots of x and $\dot{x}$ are shown in Fig. 4 and 5, respectively. From these figures, it can be seen that the given constraints are satisfied with some margin, since the controller takes into account the disturbance in (33).

If an unexpectedly large disturbance not described by Δ in (33), the state ξ may go out of the feasible regions $\mathcal{P}_i$ in (31). One simple way to deal with such infeasible problems is to apply the maximum control input outside feasible regions to recover the constraint violation as soon as possible. More systematic way for rapid recovery from constraint violation is to solve the following optimal control problem instead of (27) based on soft bounds[7]

$$\min_{\hat{\alpha}, \epsilon} \sum_{\tau=k}^{k+N-1} \hat{\alpha}^2_{[\tau|k]} + W\|\epsilon_\tau\|^2_\infty \tag{36}$$

subject to (28), (30) and

$$\underline{\xi} - \epsilon_\tau \leq \hat{\xi}_{[\tau+\ell+1|k]} \leq \overline{\xi} + \epsilon_\tau \tag{37}$$

$$0 \leq \epsilon_\tau \tag{38}$$

where W is an extremely large number. The slack variable ϵ_τ quantifies constraint violation of $\hat{\xi}_{[\tau+\ell+1|k]}$, and its non-zero value is heavily penalized in the cost function. Fig. 6 shows partitions for y direction obtained by solving (36). The upper and lower bounds of the constraints in (37) and (30) are

$$\underline{\xi}_y = \begin{bmatrix} -0.5 \\ -0.5 \end{bmatrix}, \; \overline{\xi}_y = \begin{bmatrix} 0.5 \\ 0.5 \end{bmatrix}, \; \underline{u}_y = -100, \; \overline{u}_y = 100 \tag{39}$$

Other parameters are chosen as

$$K_y = [-31.6, -148], \quad \eta = 20, \quad W = 1.0 \times 10^{10}. \tag{40}$$

V. Experiments with constraints and time delay

This section shows experimental results without disturbances. The MPC controller in x direction based on (27)-(30) is applied for the initial position $(-8, 0, 0)$. In this case, MPC controller is not necesarry in y and z direction, since the constraints are easily satisfied by LQ controllers.

The parameters for state prediction in Section III are chosen as follows:

$$G_x = G_y = G_z = \begin{bmatrix} 0 \\ 1 \end{bmatrix}, \quad \hat{\xi}_{x0} = \begin{bmatrix} x_0 \\ 0 \end{bmatrix} \tag{41}$$

$$\hat{\xi}_{y0} = \hat{\xi}_{z0} = \begin{bmatrix} 0 \\ 0 \end{bmatrix}, \quad \Lambda_x = \Lambda_y = \Lambda_z = 10 \tag{42}$$

Solid lines in Fig. 7-8 show respectively the trajectories of the position measurement x and the estimate of $\dot{x}$ for $\ell = 1$. The dash-dotted lines in Fig. 7-8 show the trajectories for $\ell = 0$, which implies that the time delay is ignored. The dash-dotted line in Fig. 8 shows that the velocity constraint is violated due to the effect of the delay. Also, the blimp is decelerated too much, since the violation penalty is imposed after the violation is recovered, because of the time delay. Fig. 9 shows that electric power is wasted for large control in the case without delay compensation. Fig. 10 using a different velocity constraint also shows constraint violation. Note that, in the case without MPC ($\alpha_x = 0$ in (25)), the experiments cannot be complited, since the velocity grows beyond the ability of the measurement system.

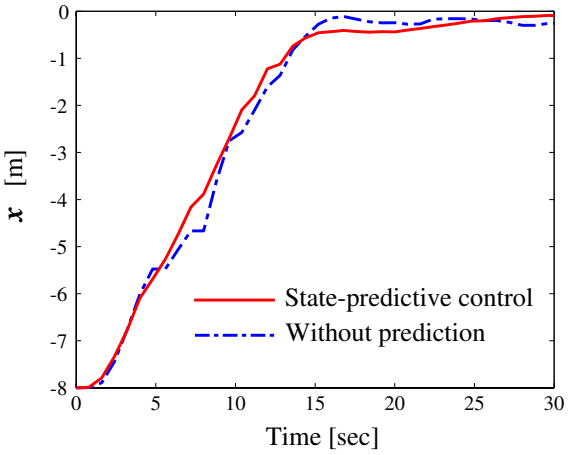

Fig. 7. Time plot of x in experiment

VI. Experiments with disturbance and time delay

This section shows experimental results in the presence of disturbance, which is the wind from a fan in y direction. In this case, the controller in (24) is replaced by the following one with additional integrator term:

$$u_{y[k]} = -K_y \hat{\xi}_{y[k+\ell|k]} + \alpha_{y[k]} - K_I \sum_{i=0}^{k} \hat{\xi}_{y[i+\ell|i]}, \tag{43}$$

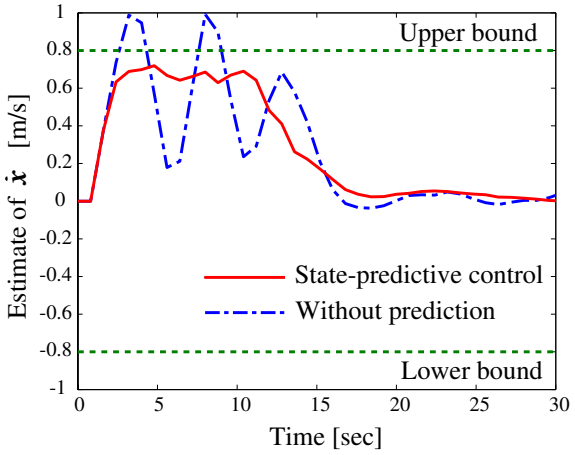

Fig. 8. Time plot of estimate of $\dot{x}$

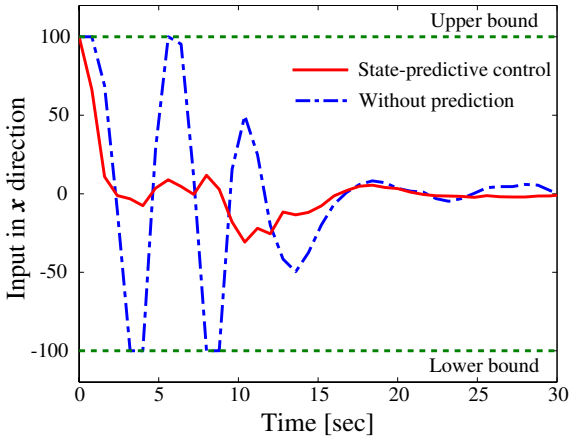

Fig. 9. Time plot of u_x

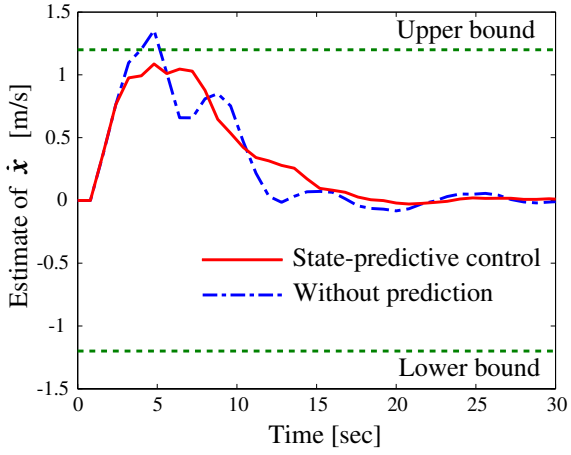

Fig. 10. Time plot of estimate of $\dot{x}$

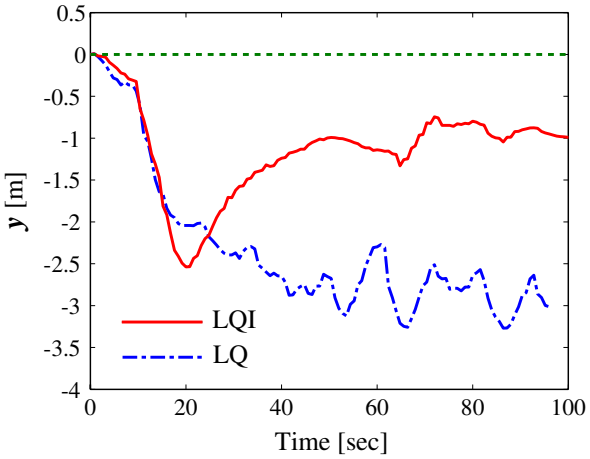

Fig. 11. Time plot of y in the presence of wind

where $\ell = 1$. Fig. 11 shows the response of y for K_y in (40) and $\alpha_{[k]} = 0$. The reponses for $K_I = 0$ and $K_I = 1$ are shown by the dash-dotted and solid lines, respectively. The parameters for state prediction are chosen as the same values in Section V. The trajectories in Fig.11 show large steady-state errors even in the case of LQI controller, due to the state prediction errors caused by the disturbance. In Fig. 12, the solid and dash-dotted lines show the position estimates by the filters in (5)-(6) and (17)-(18) for $H = B$ and $D = 0.1$, respectively. The position estimate by (5)-(6) has large error, because the bias of the disturbance is ignored. In Fig. 13, the dash-dotted and solid lines show the velocity estimates by the filters in (5)-(6) and (17)-(18), respectively. This figure shows that the velocity estimate by (5)-(6) also has large error. The solid line in Fig. 14 shows that the steady-state error is decreased by using the separate-bias filter in (17)-(18). Furthermore, Fig. 15 shows responses of y in another experiment. The dashed line shows trajectory for $\alpha_y = 0$, while the solid line shows the case of the MPC controller using the soft bound in Section IV. The separate-bias filter in (17)-(18) is used in both cases. It can be seen from Fig. 15 that the peak of the error due to the disturbance is decreased by the MPC controller using the soft bound.

VII. Conclusion

In this paper, state-predictive control is applied to an autonomous blimp in the presence of time delay and disturbance. We have constructed a state predictor to compensate time delay based on the separate-bias filters taking into account nonzero-mean disturbance. Experimental results show that constraint violations are reduced in MPC with input and state constraints by compensating time delay. Also, flight experiments in the presence of the winds show that the steady-state error to disturbances are reduced as a result that the state prediction performance is improved by using separate-bias predictor.

Acknowledgement

This research is supported in part by the Special Project for Earthquake Disaster Mitigation in Urban Areas (in cooperation with the International Rescue System Institute (IRS) and National Research Institute for Earth Science and Disaster Prevention (NIED)).

References

[1] S. B. V. Gomes and J. J. G. Ramos: Airship Dynamics Modeling for Autonomous Operation; *Proc. of the IEEE Int. Conf. on Robotics and Automation* (1998)

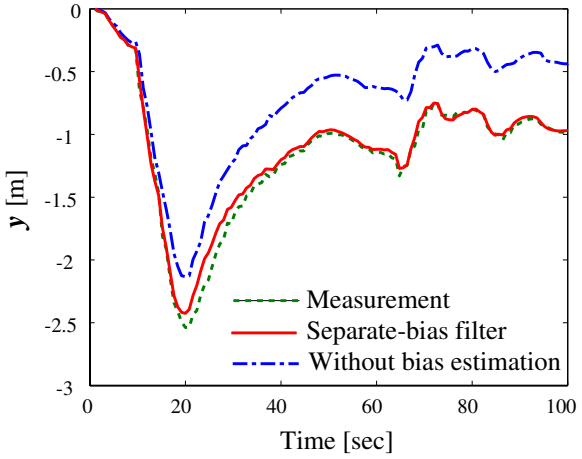

Fig. 12. Estimates of y in the presence of wind

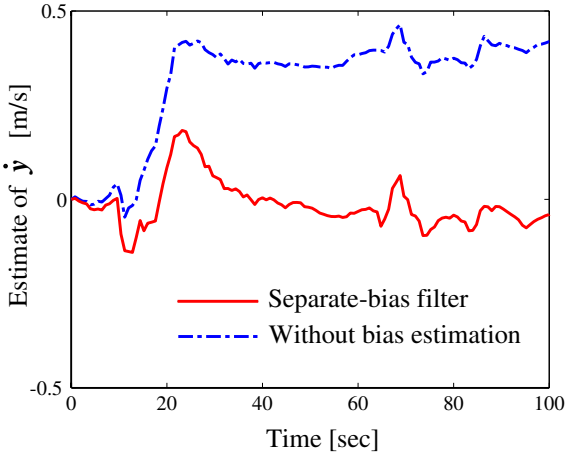

Fig. 13. Estimates of $\dot{y}$ in the presence of wind

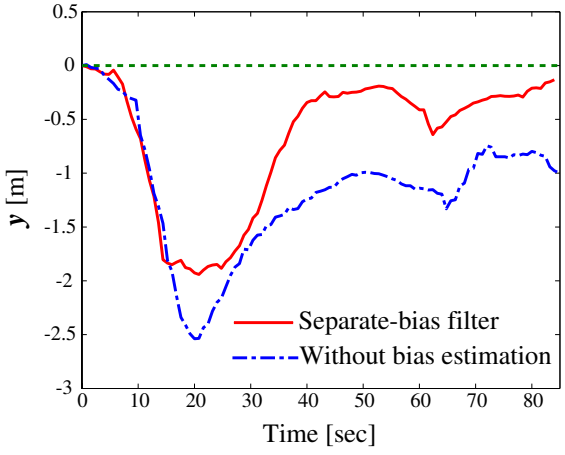

Fig. 14. Time plot of y in the presence of wind

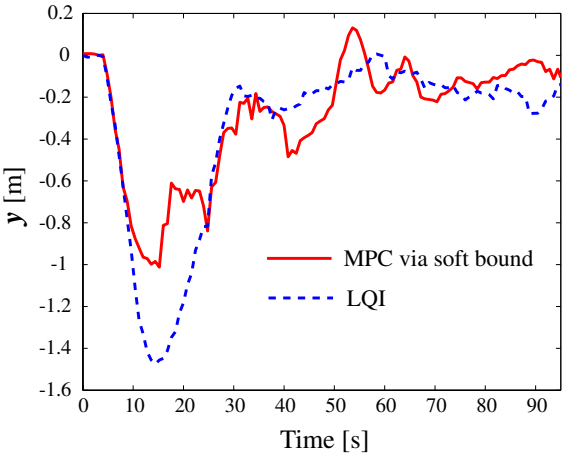

Fig. 15. Time plot of y using soft bound in MPC

[2] H. Zhang J.P. Ostrowski: Periodic Control for A Blimp-like Dynamical Robot; *Proc. of the IEEE Int. Conf. on Robotics and Automation* (2001)

[3] T. Yamasaki, K. Fujita and N. Goto: Identification of Blimp Dynamics by Constrained Flight Tests; *Proc. of AIAA Atmospheric Flight Mechanics Conference* pp. 464-474 (2001)

[4] T. Fukao, K. Fujitani and T. Kanade: Image-based Tracking Control of a Blimp; *Proc. of the 42rd IEEE Conference on Decision and Control* (2003)

[5] Yasushi Hada, Kuniaki Kawabata, Hayato Kaetsu and Hajime Asama: Autonomous Blimp System for Aerial Infrastructure; *Proc. of the 2nd Int. Conf. on Ubiquitious Robots and Intelligence Ambient Intelligence*, (2005)

[6] H. Fukushima, R. Saito, F. Matsuno, Y. Hada, K. Kawabata and H. Asama: Model Predictive Control of an Autonomous Blimp with Input and Output Constraints; *Proc. of the IEEE International Conference on Control Applications* (2006)

[7] J.M. Maciejowski : Predictive Control with Constraints; Prentice Hall (2002)

[8] A. Bemporad, M. Morari, V. Dua and E. N. Piskopoulos : The explicit linear quadratic regulator for constrained systems; *Automatica*, Vol. 38, pp. 3–20 (2002)

[9] P. Grieder, P.A. Parrilo and M. Morari: Robust Receding Horizon Control - Analysis & Synthesis; *Proc. of the 42rd IEEE Conference on Decision and Control* (2003)

[10] D.L. Kleinman; *IEEE Trans. Autom. Contr.*, Vol. 14, No. 5, pp. 524–527 (1969)

[11] E. Furutani, T. Hagiwara and M. Araki: Two-degree-of-freedom design method of state-predictive LQI servo systems; *Proc. of the 33rd IEEE Conference on Decision and Control* (1994)

[12] B. Marinescu and H. Bourlès : Robust state-predictive control with separation property: A reduced-state design for control systems with non-equal time delays; *Automatica*, Vol. 36, No. 4, pp. 555–562 (2000)

[13] B. Friedland: Treatment of Bias in Recursive filtering; *IEEE Trans. Autom. Contr.*, Vol. 14, No. 4, pp. 359–367 (1969)

[14] D. Haessig and B. Friedland: Separate-Bias Estimation with Reduced-Order Kalman Filters; *IEEE Trans. Autom. Contr.*, Vol. 43, No. 7, pp. 983–987 (1998)

[15] C. Hsieh: Robust Two-Stage Kalman Filter for Systems with Unknown Inputs; *IEEE Trans. Autom. Contr.*, Vol. 45, No. 12, pp. 2374–2378 (2000)

[16] TOPCON Electronic TotalStation: http://www.topcon.co.jp/eng/survey/st00.html

[17] G.F. Franklin, J.D. Powell and M.L. Workman : Digital Control of Dynamic Systems, Second Edition; Addison-Wesley (1990)

[18] M. Kvasnica, P. Grieder, M. Baotić and M. Morari : Multi Parametric Toolbox (MPT), http://control.ee.ethz.ch/~mpt (2004)